24th COBEM - 2017

24th ABCM International Congress of Mechanical Engineering
December 3-8, 2017, Curitiba, PR, Brazil

COBEM-2017-0549
SPRAY CONE ANGLES BY A PRESSURE SWIRL INJECTOR FOR ATOMIZATION OF GELLED ETHANOL

Gustavo Alexandre Achilles Fischer
José Carlos de Andrade
Fernando de Souza Costa
Combustion and Propulsion Laboratory - LABCP
Brazilian Institute for Space Research - INPE
Rodovia Presidente Dutra, km 40, CEP 12.630-000
Cachoeira Paulista/SP - Brazil
fischer@lcp.inpe.br

Abstract. *Gelled propellants are promising for rocket propulsion applications because they combine the advantages of solid propellants with those of liquid propellants. However, gelled propellants are more difficult to atomize than conventional liquid propellants due to their non-Newtonian behavior and higher viscosity. The application of high pressures during injection allows to reduce the viscosity and to liquefy the gelled propellant near the discharge orifice of the injector. The deformation rates within the injectors due to sudden decrease of the cross-sectional area are very large and the pseudoplasticity effect of the gels becomes essential in the process of atomization. Pressure swirl injectors are widely used in liquid rocket engines due to their high efficiency of atomization in a reduced volume. This paper presents theoretical, semi empirical and experimental results concerning the spray cone angles formed by the injection of liquid or gelled ethanol for application in rocket propulsion. Experimental data were obtained for injection of liquid ethanol and 67º INPM gelled ethanol through of the injector.*

Keywords: *pressure swirl injector, atomization, spray cone angles, gelled ethanol*

1. INTRODUCTION

The demand for high-performance and improved safety propellants for various rocket engine applications has increased during the last decades and gelled propellants seem to be a promising answer to these requirements. Gel propellant is prepared from a liquid whose rheological properties have been altered by a gelling agent and, as a result, its behavior at rest resembles that of solid propellants. In fluid mechanics, gels behave as non-Newtonian shear thinning fluids. High shear rates can lead to extensive liquefaction of gelled fluids. This liquefaction offers the possibility to design engines, which can be throttled like engines with liquid propellants, but which have simple handling and storage characteristics like engines with solid propellants (Negri and Ciezki, 2010).

The injector is responsible for the atomization of liquid propellants into the combustion chamber of a rocket engine. An efficient atomization allows to significantly increase the surface area of liquid propellants, ensuring high rates of evaporation, mixing and burning. Small droplets are required to achieve rapid ignition and establish a flame front adjacent to the injection head. Large droplets take longer to burn and thus define the length of the combustion chamber (Khavkin, 2004).

A pressure swirl injector consists of one or more inlets into a central vortex chamber, the inlets generally being tangential, thus providing the spin in the vortex chamber. Finally, the fluid emerges from an orifice in the form of a film around the periphery of the orifice; this film then breaks into a cone of spray droplets. The spray of the liquid produced at the output of this type of injector has the approximate shape of a hollow-cone (Lefebvre, 1989).

Generally, when the cone angle is increased there is also an increase in the contact of droplets of liquid injected with ambient air, which improves the atomization process, the heat and mass transfer. However, the reduction in the cone angle improves the performance of the ignition and extends the limits of stability (Ortmann and Lefebvre, 1985).

The cone angle is an important external feature of a spray. Due to the interactions of the liquid fuel with air, the spray curve has an approximate bell shape, as shown in Fig. 1, thus making difficult the measurement of the cone angle.

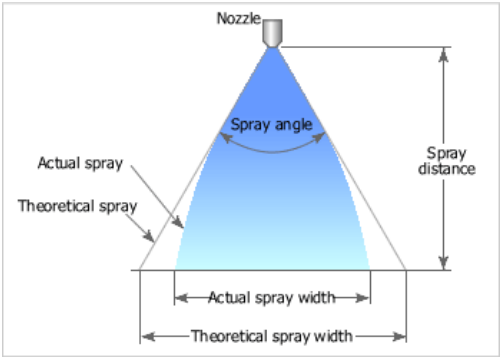

Figure 1. Spray cone angle.

The existence of yield stress and increased viscosity make gelled propellants very difficult to atomize, and restrict their wide use for aerospace applications. In Newtonian fluids, large viscosity values produce coarse sprays, and in non-Newtonian fluids shear and extensional viscosities can be several orders of magnitude larger. This results in reduced performance, and a longer combustion chamber is required (increased weight). For high combustion efficiency, fine atomization is necessary (Fu *et al.*, 2014).

The atomization of gelled propellants is significantly different from the atomization of Newtonian liquids and very little is known about the influence of rheological properties, injector geometries and working conditions on the spray pattern of gelled propellants. Although many investigations have been performed to study the spray characteristics and atomization mechanism of non-Newtonian fluids such as viscoelastic fluids etc., the spray characteristics of the gelled propellants (or power-law fluid) have yet to be studied (Fu *et al.*, 2014).

The spray cone angle is the angle α formed by two straight lines in a plane projected from the orifice discharge of injector, at a specified distance (Vásquez, 2011).

This paper compares theoretical, semi-empirical and experimental results concerning the spray cone angles formed by injection of ethanol (C_2H_6O, 95% m/m) or gelled ethanol (67º INPM) through a pressure swirl injector for application in rocket propulsion. Experimental data are obtained using photographic techniques and are analyzed by image processing software developed in MATLAB language by Vásquez (2011).

2. THEORETICAL MODEL

2.1 Ideal model

The theoretical cone angles were calculated using the approach by Abramovich, as described in detail by Fischer (2014). Figure 2 shows a scheme with a pressure swirl injector.

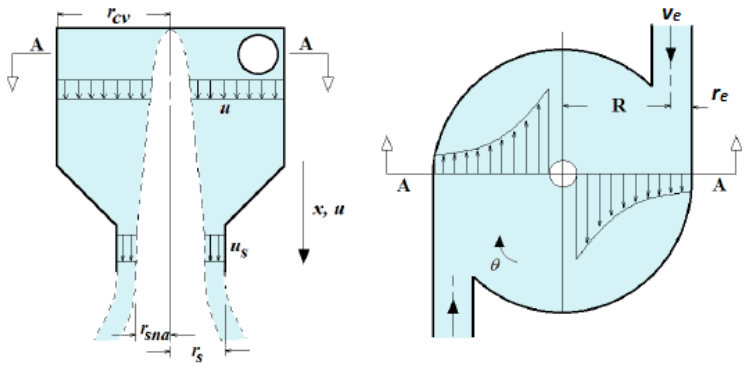

Figure 2. Scheme of a pressure swirl injector.

The characteristic geometric parameter (K) of a pressure swirl injector is defined by:

$$K = \frac{A_s\left(r_{cv} - r_e\right)}{A_e r_s} = \frac{A_s R}{A_e r_s} = \frac{\pi R r_s}{A_e} \tag{1}$$

where A_s is the area and r_s is the inner radius of the discharge orifice, A_e is the total area and r_e is the radius of tangential inlet channels, r_{cv} is the radius and R is the effective radius of the vortex chamber.

Other important parameters of the pressure swirl injectors are the liquid fraction area (ε), dimensionless radius of the gas vortex (S), discharge coefficient (μ) and spray cone angle (α). All these parameters are directly related to the K by equations (Bayvel and Orzechowski, 1993):

$$K = \frac{(1-\varepsilon)\sqrt{2}}{\varepsilon\sqrt{\varepsilon}} \tag{2}$$

$$\mu = \varepsilon\sqrt{\frac{\varepsilon}{2-\varepsilon}} \tag{3}$$

$$\tan\frac{\alpha}{2} = \frac{2\mu K}{\sqrt{(1+S)^2 - 4\mu^2K^2}} \tag{4}$$

$$\mu = \sqrt{1-\mu^2K^2} - S\sqrt{S^2-\mu^2K^2} - \mu^2K^2\ln\left(\frac{1+\sqrt{1-\mu^2K^2}}{S+\sqrt{S^2-\mu^2K^2}}\right) \tag{5}$$

A graphical solution of Eqs. (2), (3), (4) and (5) is shown in Figure 3.

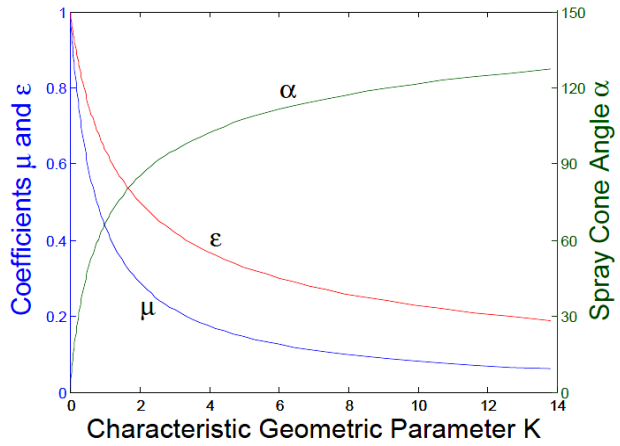

Figure 3. Behavior of the geometric characteristic parameter, discharge coefficient, liquid fraction area and spray cone angle of the pressure swirl injector.

The liquid fraction area (ε) and dimensionless radius of the gas vortex (S) are defined by:

$$\varepsilon = \frac{A_l}{A_s} = \frac{\pi\left(r_s^2 - r_{sna}^2\right)}{\pi r_s^2} = 1 - \frac{r_{sna}^2}{r_s^2} = 1 - S^2 \tag{6}$$

$$S = \frac{r_{sna}}{r_s} = \sqrt{1-\varepsilon} \tag{7}$$

where A_l is the area occupied by liquid and r_{sna} the gas core radius in the discharge orifice.

2.2 Model considering viscous losses

The theoretical model used here for the flow of viscous liquid into a pressure swirl injector is based on the Kliachko approach (Borodin *et al.*, 1967). The characteristic geometric parameter considering the viscous effects (K_λ) must be corrected by equation:

$$K_\lambda = \frac{Rr_s}{\frac{A_e}{\pi} + \left(\frac{\lambda}{2}\right)R(R-r_s)} = \frac{K}{1+\left(\frac{\lambda}{2}\right)\left(B^2-K\right)} \tag{8}$$

where $B = R\sqrt{\pi/A_e}$.

where the coefficient of friction (λ) is a function of Reynolds number (*Re*) of the tangential inlet channels obtained from the following equation:

$$\log\lambda = \frac{25{,}8}{(\log \mathrm{Re})^{2{,}58}} - 2 \tag{9}$$

Equation (9) for a pressure swirl injector is valid for $\mathrm{Re} = 10^3 - 10^5$. The values determined from this equation are significantly higher than from other equations commonly used in hydraulic systems (Bazarov *et al.*, 2004).

Thus, it is possible to recalculate the liquid fraction area (ε_λ) and the dimensionless radius of the gas vortex (S_λ) considering the viscous effects by Eqs. (2) and (7), respectively.

The friction of the liquid on the vortex chamber wall causes a decrease of the angular motion and energy losses. For a more precise calculation of the pressure drop it is necessary to consider the energy losses in the pressure swirl injector. In the vortex chamber of an injector these losses can be considered as the work of the frictional force along the trajectory of the liquid. Thus, the corrected discharge coefficient (μ_λ) is calculated by:

$$\mu_\lambda = \frac{1}{\sqrt{\dfrac{K_\lambda^2}{1-\varepsilon_\lambda} + \dfrac{1}{\varepsilon_\lambda^2} + \xi_i \dfrac{K^2}{C^2} + \Delta}} \tag{10}$$

where $C = R/r_s$, $\xi = 1/K + \lambda C/2$ and:

$$\Delta = \frac{\lambda}{\xi^2}\left\{\frac{1}{\xi}\left(1-\frac{1}{C}\right) + \lambda\left[\frac{K^2}{4} - \frac{1}{(2\xi-\lambda)^2} + \frac{K}{\xi} - \frac{2}{\xi(2\xi-\lambda)} + \frac{3}{2\xi^2}\ln\left(\frac{(2\xi-\lambda)KC}{2}\right)\right]\right\} \tag{11}$$

The friction coefficient through the tangential inlet channels depends on the Reynolds number (*Re*):

$$\mathrm{Re} = \frac{4\dot{m}}{\pi\mu_l\sqrt{n}d_e} \tag{12}$$

where $\dot{m}$ is the mass flow rate, d_e is the diameter and n the number of tangential inlet channels and μ_l is the dynamic viscosity of the fluid.

The total friction loss in the tangential channels (ξ_i) is computed by:

$$\xi_i = \xi_e + \lambda\frac{l_e}{d_e} \tag{13}$$

where the initial loss coefficient, ξ_e, is determined from Fig. 3, and the inclination of the tangential inlet channels, α_e, is obtained from:

$$\alpha_e = 90^o - \tan^{-1}\left(\frac{r_{cv}}{l_e}\right) \tag{14}$$

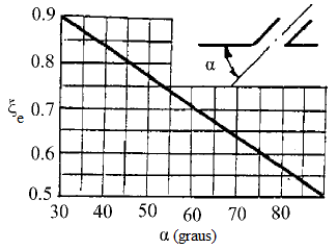

Figure 3. Initial viscous loss coefficient versus inclination of tangential inlet channels.

The corrected spray cone angle (α_λ) is calculated considering the effects of geometry and friction losses:

$$\tan\frac{\alpha_\lambda}{2}=\frac{2\mu_\lambda K_\lambda}{\sqrt{(1+S_\lambda)^2-4\mu_\lambda^2K_\lambda^2}} \tag{15}$$

2.3 Semi empirical models

Rizk and Lefebvre (Lefebvre, 1989) considered the effects of liquid properties, geometrical parameters, and injection pressure on the liquid film thickness, and derived the following equation for the spray angle:

$$\frac{\alpha}{2}=6K^{0,15}\left(\frac{\Delta P d_s^2\rho}{\mu_l^2}\right)^{0,11} \tag{16}$$

Benjamin (1998) validated an equation using a database and modified the coefficients indicated by Rizk and Lefebvre (Lefebvre, 1989) for large size injectors and obtained:

$$\frac{\alpha}{2}=9.75K^{0,287}\left(\frac{\Delta P d_s^2\rho}{\mu_l^2}\right)^{0,067} \tag{17}$$

2.4 Generalized Reynolds number for non-Newtonian fluids

To characterize or to compare the flow characteristics of fluids flowing through ducts, dimensionless numbers are often used. The Reynolds number for a Newtonian fluid can be written as

$$\mathrm{Re}=\frac{\rho d\bar{u}}{\mu} \tag{18}$$

where ρ is the fluid density, d is the duct diameter, $\bar{u}$ is the average flow velocity, and μ is the constant Newtonian viscosity.

The rheological behavior of a gel is commonly described in the simplest form by the Ostwald-de-Waele or power-law (PL) equation:

$$\eta_{PL}=K\dot{\gamma}^{n-1} \tag{19}$$

where η and $\dot{\gamma}$ denote the shear viscosity and shear rate, respectively. K is called "consistency coefficient" and n is the flow index.

For the identification of different flow regimes, Metzner and Reed (1955) introduced a generalized Reynolds number valid for pure PL liquids. This number was derived from its relation to the Darcy friction factor and is given by:

$$\mathrm{Re}_{GEN-PL}=\frac{\rho d^n\bar{u}^{2-n}}{K\left((3n+1)/4n\right)^n 8^{n-1}} \tag{20}$$

In the present work, the friction coefficient λ_{PL} for non-Newtonian fluids was assumed a function of the generalized Reynolds number $\mathrm{Re}_{GEN\text{-}PL}$ of the tangential inlet channels, obtained from the following equation:

$$\log\lambda_{PL}=\frac{25{,}8}{(\log\mathrm{Re}_{GEN-PL})^{2,58}}-2 \tag{21}$$

3. EXPERIMENTAL METODOLOGY

A pressure swirl injector of gelled ethanol was designed for application in rocket engines, based on the methodology described by Fischer (2014).

The experimental system consists of a gel tank, injector, pressure and flow rate measurement system and a high-speed camera. A pressurized supply system was adopted. The gel simulant is fed into the injector by a piston in the tank.

3.1 Rheological characterization

The 67° INPM gelled ethanol obtained commercially was used as surrogate in the experiments, instead of gelled anhydrous ethanol. The physical properties of gel are presented in Table 1:

Table 1 – The physical properties of 67° INPM gelled ethanol.

Physical Properties	***Minimum***	***Maximum***
Alcohol content (w/w) °INPM	69.55	75.27
Alcohol content (w/w) °GL	76.9	81.4
pH	6	8
Density (kg/m³) at 20°C	850	860
Viscosity (cP), in rest, at 20°C	>12,000	

The rheological properties of the test fluid were characterized using a Brookfield cone-and-plate controlled stress rotational viscometer (CAP 200 model), with a 1.2 cm diameter and 1.8° truncated cone. Figure 4 shows the shear rheology for the 67° INPM gelled ethanol at 50°C.

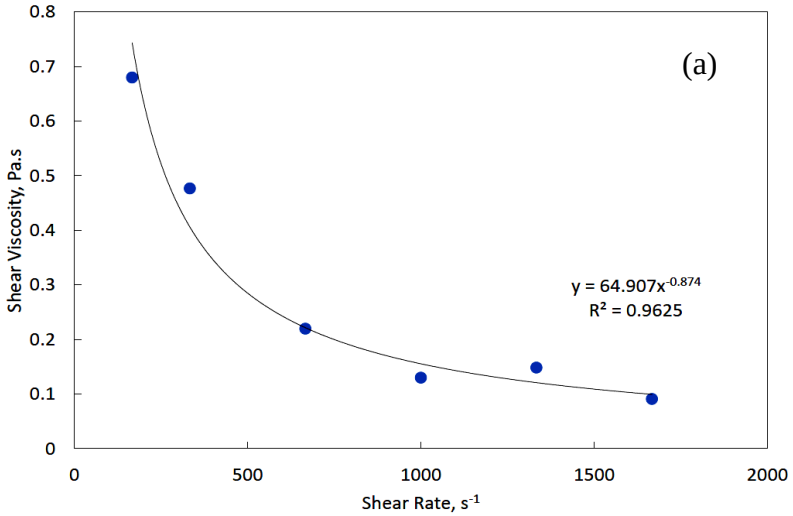

Figure 4. Rheological characterization of 67° INPM gelled ethanol.
(a) shear viscosity vs shear rate; (b) rotational viscometer.

The rheological behavior of the gel is commonly described by Eq. (19). From the rheological curve, we can obtain K = 64.907 Pa.s^n and n = 0.126.

3.2 The pressure swirl injector

Table 2 shows a general overview of the pressure swirl injector dimensions. Table 3 presents a general overview of the operational and geometric parameters for design of the pressure swirl injector, respectively.

Table 2. General overview of the pressure swirl injector dimensions.

Injector dimensions	Values
Diameter of the discharge orifice – d_s (mm)	1.6
Length of the discharge orifice – l_s (mm)	8.1
Number of the tangential inlet channels – n	2
Diameter of the tangential inlet channels – d_e (mm)	1.4
Length of the tangential inlet channels – l_e (mm)	2.8
Effective radius of the vortex chamber – R (mm)	3.3
Diameter of the vortex chamber – D_{cv} (mm)	8
Length of the vortex chamber – L_{cv} (mm)	4.2
Transient cone angle – β (°)	90

Table 3. Characteristics of the pressure swirl injector tested.

Input data		
Pressure drop – ΔP (MPa)	0.2533	
Mass flow rate – $\dot{m}$ (g/s)	10.0538	
Spray cone angle – α (º)	90	
Work fluid	Ethanol	Gelled Ethanol
Dynamic viscosity – μ_l (cP)	1.2	-
Density – ρ (kg/m³)	809.3	855

Injector parameters				
	No viscosity		With viscosity	
Work fluid	Ethanol	Gelled Ethanol	Ethanol	Gelled Ethanol
Friction coefficient (λ)	0	0	0.073	0.1626
Reynolds number (Re)	0	0	5391.8	1645.5
Spray cone angle – α (º)	90	90	82.2085	74.6441
Discharge coefficient (μ)	0.2226	0.2226	0.264	0.3062
Liquid fraction area (ε)	0.4271	0.4271	0.4808	0.5328
Characteristic geometrical parameter (K)	2.9028	2.9028	2.2028	1.6993
Dimensionless radius of the gas vortex (S)	0.8272	0.8272	0.7689	0.7162
Total injection velocity – V (m/s)	5.5683	5.0093	6.6042	7.4525
Mass flow rate – $\dot{m}$ (g/s)	10.0538	10.0538	11.9241	13.8304

Figure 4 shows a picture of the manufactured injector.

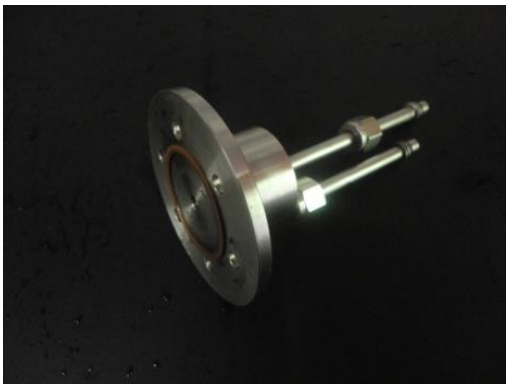

Figure 4. Picture of the manufactured injector.

3.3 Spray angle measurement

The experimental setup used for measuring the spray cone angle by photographic techniques consists of a support to fix the injector on the test bench and a digital camera. The pictures were obtained by a Sony DSC-F828 digital camera, with 8 megapixels of effective resolution, or 3264×2448 pixels. The support has a mark that serves to indicate a known length to be used as a reference to relate the number of pixels and the true length of the image, allowing determine the experimental values of the spray cone angles from the respective images.

Figure 5 shows the GUI (Graphical User Interface) developed in MATLAB language by Vásquez (2011), especially written for this work to process spray images. The use of this GUI is relatively simple and the images can be treated in JPEG, TIFF or BMP formats.

After taking and selecting the appropriate images, the image processing is done with the GUI developed for this purpose. Finally, the experimental values of the spray cone angles of these images are registered. After data collection and treatment, the experimental curves are obtained and compared to the theoretical data.

Figure 5. GUI for image processing.

4. RESULTS AND DISCUSSIONS

Figure 6 compares the theoretical and experimental values of the mass flow rates of ethanol and gelled ethanol versus injection pressure.

Figures 7 and 8 show, respectively, the discharge coefficients and spray cone angles versus the mass flow rates of the ethanol and gelled ethanol.

The test fluids used in all experiments were liquid ethanol (C_2H_6O, 95% m/m) and gelled ethanol (67º INPM), respectively.

As seen in Figure 6a, experimental mass flow rates of liquid ethanol match the analytical solution with viscous effects for manometric injection pressures between 1 and 2.5 bar. The design point corresponds to 10 g/s and 2.2 bar with viscous losses. Smaller mass flow rates result in larger loss of angular momentum causing a discrepancy between the analytical solution and experimental data whereas larger mass flow rates produce lower angular momentum losses and, therefore, theoretical values depart from experimental ones.

Flow of gelled ethanol started at injection pressures about 1.5 bar, with formation of a liquid jet, while initial spray formation occurred only above injection pressures above 1.3 bar, approximately. A good gel atomization efficiency occurred for injection pressures above 4 bar, approximately. Figure 6b shows gel injection pressures varying from 1.3 to 9.5 bar while mass flow rates increase from 14 to 33 g/s. Due to the viscosity of the gelled ethanol (about 0.12 Pa.s or 120 cP for a shear rate of 1500 s^{-1}) be about a hundred times larger than that of liquid ethanol (1.2 cP), the initial energy required to move the fluid is also greater.

As seen in Figs. 7a, the experimental discharge coefficients for injection of liquid ethanol had good agreement with the analytical solution with viscous losses in most of the operating range, from 7 to 14 g/s, except at low mass flow rates as mentioned above.

As seen in Figs. 7b, the discharge coefficient of gelled ethanol was more than two times higher than the estimated value over the entire operating range. Although the coefficient of friction determined by the proposed model is significantly higher than that of other equations commonly used in hydraulic systems, for the case of non-Newtonian fluids, it is verified experimentally that the viscous effects are still underestimated and consequently the values obtained for the discharge coefficients were lower than in practice.

As seen in Fig. 8a, the Benjamin semi-empirical formulation provided the best estimated of the spray cone angle of liquid ethanol. The analytical solution considering the viscous effects has good agreement with experimental data, but was 16% lower in the project condition (10 g/s). This is expected, since the theoretical solution is a function only of the injector parameters and does not consider the fluid properties and operating conditions. Another relevant fact is that analytical solution does not consider the length of the vortex chamber and discharge orifice.

As seen in Figs. 8b, the semi-empirical models could not be used for the gelled ethanol, because they do not consider the effect of the rheological properties of the non-Newtonian fluids on the flow in the pressure swirl injector. The analytical solution considering the viscous effects has good agreement with experimental data above a mass flow rate of 26 g/s with a slight discrepancy around 19% higher than the values obtained experimentally. This is expected due to the same explanations mentioned above. Spray formation was observed only above 26 g/s.

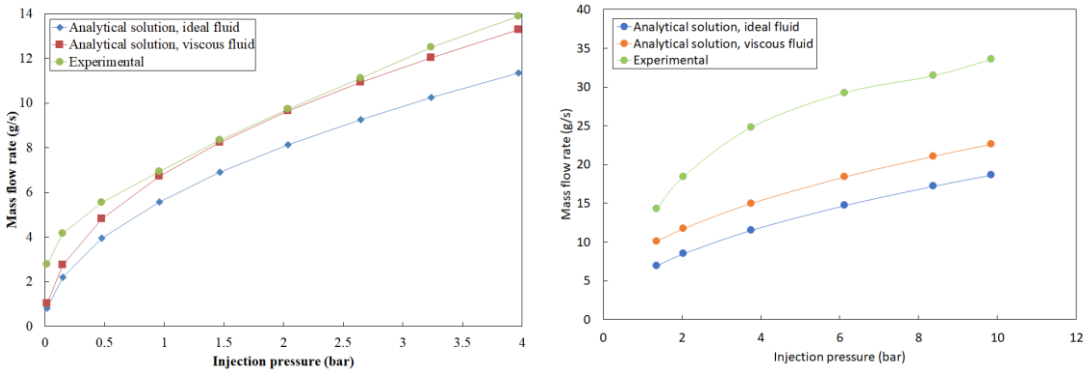

a) Ethanol b) Gelled Ethanol

Figure 6. Theoretical and experimental values of the mass flow rate of ethanol and gelled ethanol versus pressure injection (gauge) in the pressure swirl injector.

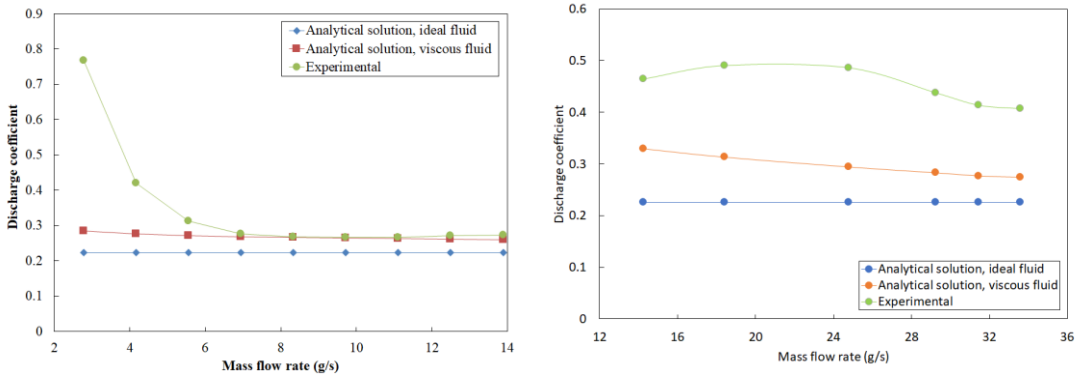

a) Ethanol b) Gelled Ethanol

Figure 7. Theoretical and experimental values of the discharge coefficient versus mass flow rate of the ethanol and gelled ethanol in the pressure swirl injector.

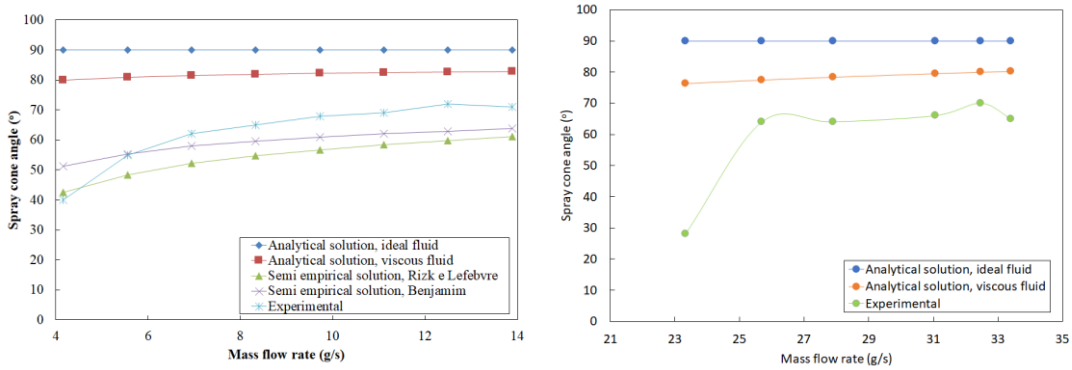

a) Ethanol b) Gelled Ethanol

Figure 8. Theoretical, semi-empirical and experimental values of the spray cone angle of ethanol and gelled ethanol versus mass flow rate in the pressure swirl injector.

5. CONCLUSIONS

Theoretical and semi-empirical spray cone angles for injection of ethanol and gelled ethanol in a pressure swirl injector were calculated and compared to experimental data. A graphical user interface was used to determine spray cone angles from spray images.

The discharge coefficients of the pressure swirl injector had good agreement with the analytical solution considering the viscous effects for most of the operating range using liquid ethanol. For the case of gelled ethanol, the discharge coefficient was higher than estimated over the entire operating range, which means that the model proposed for the calculation of the coefficient of friction cannot accurately estimate the behavior of the non-Newtonian fluid. Further studies are needed for the development of new empirical or semi empirical models that more accurately represent the internal flow of non-Newtonian fluids in pressure swirl injectors.

The semi-empirical models could not be used for gelled ethanol in the pressure swirl injector, because they do not consider the rheological properties of non-Newtonian fluids on the flow in the pressure swirl injector.

The Benjamin semi-empirical formulation provided the best estimates of spray cone angles for injection of liquid ethanol in the pressure swirl injector, thus indicating that both liquid physical properties and injector geometry are important to determination this parameter.

6. ACKNOWLEDGEMENTS

The authors thank FAPESP for support through the process 2016 / 21957-0 and CNPq for the PhD scholarship granted to the first author.

7. REFERENCES

Bayvel, L. and Orzechowski, Z., 1993. “Liquid Atomization”, Taylor & Francis, Washington, DC.

Bazarov, V.; Vigor, Y. and Puri, P., 2004. “Design and dynamics of jet and swirl injectors, liquid rocket thrust chambers: aspects of modeling, analysis, and design”. United States of America: American Institute of Aeronautics and Astronautics.

Borodin, V.A.; Dityakin, Yu.F.; Klyachko, L.A. and Yagodkin, V.L., 1967. “Liquid Atomization”, Mashinostroenie, Moscow.

Fischer, G.A.A., 2014. “Injetores centrífugos duais e jato-centrífugos para aplicação em propulsão de foguetes”, Master thesis, Instituto Nacional de Pesquisas Espaciais, São José dos Campos, SP, Brazil.

Fu, Q., Duan, R., Cui, K. and Yang, L., 2014. “Spray of gelled propellants from an impingement-jet injector under different temperatures”, *Aerospace Science and Technology*, Vol. 39, No. 1, pp. 552-558.

Giffen, E. and Muraszew, A., 1953. “Atomization of Liquid Fuels”, Chapman and Hall, London.

Khavkin, Y.I., 2004. “Theory and practice swirl atomizers”, Taylor & Francis, New York.

Kulagin, L.V. and Okhotnikov S.S., 1970. “Combustion of Heavy Liquid Fuels”, Mashinostroenie, Moscow.

Lefebvre, A.H., 1989. “*Atomization and Sprays*”, Hemisphere, New York.

Madlener, K., Frey, B., and Ciezki, H.K., 2007. “Generalized Reynolds Number for non-Newtonian Fluids”, *2nd European Conference for Aerospace Sciences* (EUCASS2007), Brussels, Belgium.

Metzner, A.B. and Reed, J.C., 1955. “Flow of non-Newtonian fluids – correlation of the laminar, transition and turbulent-flow regios”. AIChE J., Vol. 1, No. 4, pp. 434-440.

Natan, B. and Rahimi, S., 2001. “The status of gel propellants in year 2000”, in K. K. Kuo and L. DeLuca, Eds., *Combustion of Energetic Materials*, Begell House, New York, pp. 172-194.

Negri, M. and Ciezki, H.K., 2010. “Atomization of non-Newtonian Fluids with and Impinging Jet Injector: Influence of Viscoelasticity on Hindering Droplets Formation”, AIAA Paper 2010-6821.

Ortmann, J. and Lefebvre, A.H., 1985. “Fuel Distributions from Pressure-swirl Atomizers”, *Journal Propulsion and Power*, Vol. 1, No. 1, pp. 11-15.

Vásquez, R.A., 2011. “Desenvolvimento de um injetor centrífugo dual para biocombustíveis líquidos”, Master Thesis, Instituto Nacional de Pesquisas Espaciais, São José dos Campos, SP, Brazil.

Yang, L., Fu, Q., Zhang, W., Du, M. and Tong, M., 2011. “Atomization of Gelled Propellants from Swirl Injectors with Leaf Spring in Swirl Chamber”, *Atomization and Sprays*, Vol. 21, No. 11, pp. 949-969.

Yang, L., Fu, Q., Qu, Y., Zhang, W., Du, M. and Xu, B., 2012. “Spray Characteristics of Gelled Propellants in Swirl Injectors”, *Fuel*, Vol. 97, pp. 253-261.

8. RESPONSIBILITY NOTICE

The authors are the only responsible for the printed material included in this paper.